Reexamining the Near-Core Radial Structure of the Tropical Cyclone Primary Circulation: Implications for Vortex Resiliency

KEVIN J. MALLEN*

Department of Meteorology, University of Hawaii at Manoa, Honolulu, Hawaii

MICHAEL T. MONTGOMERY

Department of Atmospheric Science, Colorado State University, Fort Collins, Colorado

BIN WANG

International Pacific Research Center and Department of Meteorology, University of Hawaii at Manoa, Honolulu, Hawaii

(Manuscript received 9 January 2003, in final form 23 July 2004)

ABSTRACT

Recent theoretical studies, based on vortex Rossby wave (VRW) dynamics, have established the importance of the radial structure of the primary circulation in the response of tropical cyclone (TC)–like vortices to ambient vertical wind shear. Linear VRW theory suggests, in particular, that the degree of *broadness* of the primary circulation in the near-core region beyond the radius of maximum wind strongly influences whether a tilted TC vortex will realign and resist vertical shear or tilt over and shear apart. Fully nonlinear numerical simulations have verified that the vortex resiliency is indeed sensitive to the initial radial structure of the idealized vortex. This raises the question of how well the "true" nature of a TC's primary circulation is represented by idealized vortices that are commonly used in some theoretical studies.

In this paper the swirling wind structure of TCs is reexamined by utilizing flight-level observations collected from Atlantic and eastern Pacific storms during 1977–2001. Hundreds of radial profiles of *azimuthal-mean* tangential wind and relative vorticity are constructed from over 5000 radial flight leg segments and compared with some standard idealized vortex profiles. This analysis reaffirms that real TC structure in the near-core region is characterized by relatively slow tangential wind decay in conjunction with a *skirt of significant cyclonic relative vorticity* possessing a negative radial gradient. This broadness of the primary circulation is conspicuously absent in some idealized vortices used in theoretical studies of TC evolution in vertical shear. The relationship of the current findings to the problem of TC resiliency is discussed.

1. Introduction

a. Motivation

The radial structure of the tropical cyclone (TC) primary circulation appears to be important in the prediction of the TC vortex response to environmental vertical wind shear. The importance of moist convective processes in the intensification and maintenance of axisymmetric TCs is now well known and reasonably understood (e.g., Ooyama 1969; Rotunno and Emanuel 1987). Recent theoretical studies, however, have attempted to elucidate the role that dry-adiabatic dynamics play in the nonaxisymmetric vortex response to impinging vertical shear. Using initially barotropic vortices, Jones (1995, hereafter J95) showed that an initially tilted vortex tends to resist vertical shear by cyclonically precessing upshear and tilting over slowly in comparison to the time scale of the differential advection. The fact that most of the vortices in J95 eventually succumb to weak vertical shear (4 m s^{-1} per 10 km) may be misinterpreted that moist convective processes are essential for maintaining upright TCs in realistic environments with impinging vertical shear. Although a cyclonic precession also occurred in the dry-adiabatic vortex-in-shear simulations of Reasor et al. (2004, hereafter RMG), in contrast to J95, the barotropic vortices employed by RMG remained vertically coupled in a nearly upright configuration. The results of RMG suggest that even without moist processes TC-like vor-

* Current affiliation: Department of Atmospheric Science, Colorado State University, Fort Collins, Colorado.

Corresponding author address: Kevin J. Mallen, Department of Atmospheric Science, Colorado State University, Fort Collins, CO 80523.
E-mail: kmallen@atmos.colostate.edu

tices are more resilient to vertical shear than previously believed. The source of the discrepancy between the vortex simulations in J95 and RMG was the initial specification of the primary circulation. Why, then, is the radial structure of the primary circulation so important in supporting vortex resiliency to vertical shear?

b. Review of vortex resiliency theory

Recent theoretical studies explain, from different perspectives, the evolution of an initially tilted or vertically sheared geophysical vortex using vortex Rossby wave (VRW) theory (Reasor and Montgomery 2001; Schecter et al. 2002; RMG; Schecter and Montgomery 2003, hereafter SM1; Schecter and Montgomery 2004, hereafter SM2). In the linear VRW formalism, the precession of the vortex and its alignment can be represented as the propagation and amplitude decay of VRW disturbances that propagate on the radial potential-vorticity-gradient waveguide of the azimuthal-mean vortex. For simplicity, the initial vortex is assumed to be barotropic. Depending on the mean vortex Rossby number and the ratio of the horizontal scale of the vortex to the far-field internal Rossby deformation radius, the tilt decay for TC-like vortices occurs either via outward-propagating sheared VRW disturbances or resonance damping of a VRW quasi mode (see RMG for further details).

The sheared route of tilt decay is analogous to the familiar Thomson/Orr decay mechanism for sheared disturbances (Thomson 1887; Orr 1907; Montgomery and Kallenbach 1997; McWilliams et al. 2003). The resonant-damping route of tilt decay (Briggs et al. 1970) can be demonstrated analytically for the particular case of a Rankine-with-skirt vortex (Fig. 1) in which the nonzero "skirt" of vorticity outside the core represents a perturbation from a Rankine vortex in the sense that the peripheral circulation is small compared to that of the vortex core (Schecter et al. 2002; SM1). In the resonant damping route the tilt decay rate is proportional to the negative radial gradient of Rossby–Ertel potential vorticity (PV) (Hoskins et al. 1985) at a *critical radius* beyond the radius of maximum azimuthal-mean tangential wind (RMW), where the precession frequency of the vortex tilt matches the rotation rate of the mean azimuthal flow.

Linear VRW theory includes the possibility of a growing tilt asymmetry. If the radial PV gradient is positive at the critical radius then the VRW representing the tilt asymmetry will grow exponentially in time, with an *e*-folding time scale that is comparable to the advective time scale of the vortex core (Schecter et al. 2002; RMG; SM1; SM2; Gent and McWilliams 1986). RMG demonstrated that this indeed occurred for the "standard" vortex profile used in the J95 benchmark simulation. This standard vortex, in addition to weaker versions that retain the same nondimensional shape, form a class of idealized vortex profiles based upon Smith (1990, henceforth termed *S90 vortices*; see Fig. 1)

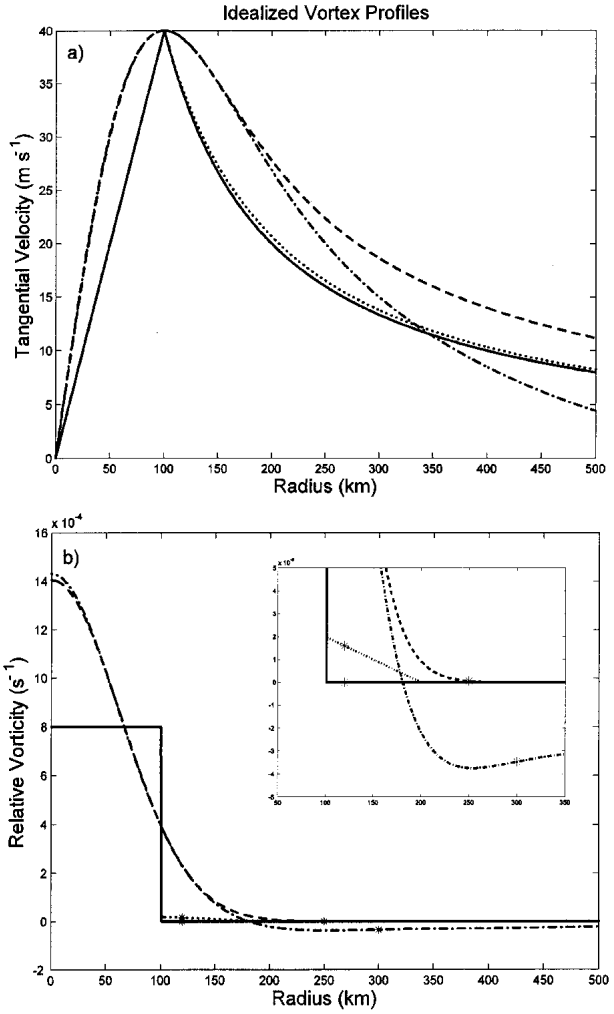

FIG. 1. Idealized radial profiles of (a) tangential velocity and (b) relative vorticity for the Rankine (solid), Rankine-with-skirt (dotted), Gaussian (dashed), and S90 (dash–dot) vortices for $\overline{V}_{\max}$ = 40 m s^{-1} and RMW = 100 km. See appendix for the analytic expressions. The critical radii (asterisk) for the Rankine and Rankine-with-skirt vortices are calculated from analytic formulations derived in SM1, and were estimated for Gaussian and S90 vortices in RMG.

that were utilized in 9 out of 10 J95 simulations and 2 of the 4 simulations in Jones (2000). Here, the positive radial PV gradient at the critical radius of the S90 vortex and consequent "tilt instability" originates from the transition of cyclonic to anticyclonic relative vorticity not far beyond the RMW. In contrast to J95, the tilted vortices in RMG realigned because the family of vortices considered there, including the Gaussian PV distribution (Fig. 1), possessed monotonically decreasing radial distributions of positive PV and consequently, sufficiently *negative* radial PV gradients at the critical radius.

The tilt asymmetry can also grow in amplitude by a vortex-Rossby/inertia–buoyancy (RIB) wave instability. If the rotation rate of the core is sufficiently large compared to the Coriolis frequency, and if the mean

radial PV gradient at the critical radius is sufficiently weak (or zero, as in the case of a pure Rankine vortex, see Fig. 1), VRW-induced phase mixing centered at the critical radius is insufficient to suppress a frequency matching with an outward-propagating inertia–buoyancy wave. The composite RIB disturbance yields an exponentially growing core tilt asymmetry whose *e*-folding time scale can again be comparable to the advective time scale of the vortex core (SM2; cf. Plougonven and Zeitlin 2002 and Ford 1994). A sufficiently negative radial PV gradient at the critical radius, however, can suppress this instability altogether (according to linear theory), preserving asymmetric balanced flow and maintaining a nearly erect vortex (RMG; SM2).

Clearly, the stable or unstable vortex response to vertical wind shear in these idealized (adiabatic) TC models is critically dependent on its radial structure. As a side note, we believe it is worth pointing out that the sheared TC problem shares some similarities with the problem of two-dimensional disk stability in astrophysical hydrodynamics. In accretion disks, the sensitivity to the radial structure of the vortex and the influence of the mean radial PV gradient in suppressing radiative (acoustic) instabilities has been known for some time (Papaloizou and Pringle 1987; cf. Plougonven and Zeitlin 2002). For geophysical vortices the Mach numbers are generally small compared to unity and acoustic coupling is negligible on advective time scales of interest; inertia–gravity waves are the pertinent "acoustic modes" in this case. These ideas have recently been synthesized using angular pseudomomentum concepts (SM2).

When moist processes are included, the sheared TC problem becomes more complicated. But RMG argue (their section 1) that the tilt dynamics is still controlled in a first approximation by dry adiabatic dynamics. When a hurricane-strength barotropic vortex with a realistic Rossby deformation radius is subject to a simple tilt perturbation (azimuthal and vertical wavenumber-one asymmetry, see Fig. 3 from Reasor and Montgomery 2001), the critical radius is found to lie between one and four RMW distances (SM1; RMG). Guided by accepted reasoning that moist processes in the eyewall region give rise to a reduced effective static stability (e.g., Emanuel et al. 1987; Montgomery and Farrell 1992; Shapiro and Montgomery 1993), the critical radius should reside radially inward from its dry estimate (Reasor et al. 2000, their section 5). Since precise critical radii for various tilt perturbations have not yet been determined for the moist convective problem, we adopt here a conservative approach assuming that the moist critical radius lies between 1–3 RMW distances for the vertically averaged axisymmetric vortex.

c. Review of TC radial structure

The foregoing discussion naturally raises important questions for the TC problem: In theoretical studies, how realistic are the idealized vortex profiles used in representing the radial structure of the TC primary circulation? What is the true radial structure of the TC primary circulation?

Keeping in mind that the preceding theoretical discussion concerns the resiliency of initially barotropic TC-like vortices in a PV framework, we would ideally prefer to estimate the radial distribution of the vertically averaged axisymmetric PV from observations of the full three-dimensional kinematic and thermodynamic structure of TCs. In the most comprehensive analyses of a single TC performed to date, Shapiro and Franklin (1995) calculated PV for the vortex core and environment of Hurricane Gloria (1985) from a multitude of data sources, such as Omega dropwindsondes (ODWs), Doppler radar, and various synoptic datasets. The radial-height cross section of Gloria's azimuthal-mean PV structure (from Shapiro and Franklin 1995) and tangential wind (from Franklin et al. 1993) are shown in Fig. 2. Throughout the troposphere, positive PV (Fig. 2a) decreases radially outward to approximately 250 km, except inward of the secondary PV maximum located at midlevels near 100-km radius and at the highest levels of the core region. Beyond the 250-km radius, the troposphere is characterized by weak PV gradients (negative and positive). Since the tangential wind maximum throughout the tropospheric depth is located near the 20-km radii (Fig. 2b), the critical radius is likely to reside somewhere between 20–60 km, a region of negative PV gradient for the vertically averaged vortex. On the basis of the foregoing discussion, we would thus expect Hurricane Gloria to remain resilient to vertical shear in weak to moderately sheared environments.

Unfortunately, the kinematic and thermodynamic data necessary for the calculation of PV throughout the tropospheric depth is not widely available, Gloria (1985) being the notable exception. There exists, however, a wealth of knowledge of TC structure based on observations of the swirling circulation, prior to the popularization of PV dynamics in TC studies.

Historically, the primary circulation has been a particular focus of many TC studies. Depperman (1947) was apparently the first to apply the Rankine vortex to approximate the TC primary circulation. The Rankine vortex is characterized by solid-body rotation within the RMW and conserved relative angular momentum outside (i.e., Vr = constant) (e.g., Batchelor 1967). The frictional loss of cyclonic relative angular momentum of inward spiraling boundary layer air observed in TCs, however, required a modification to the Rankine vortex, Vr^{α} = constant where the decay component $\alpha < 1$ (Hughes 1952; Riehl 1954). Riehl (1963), and more recently Pearce (1993), have argued theoretically that with the typical specification of boundary layer frictional drag, $F \sim V^2$, the tangential wind speed (V) in *steady-state* mature hurricanes must decrease with radial distance (r) as $V \sim r^{-1/2}$. This was elegantly dem-

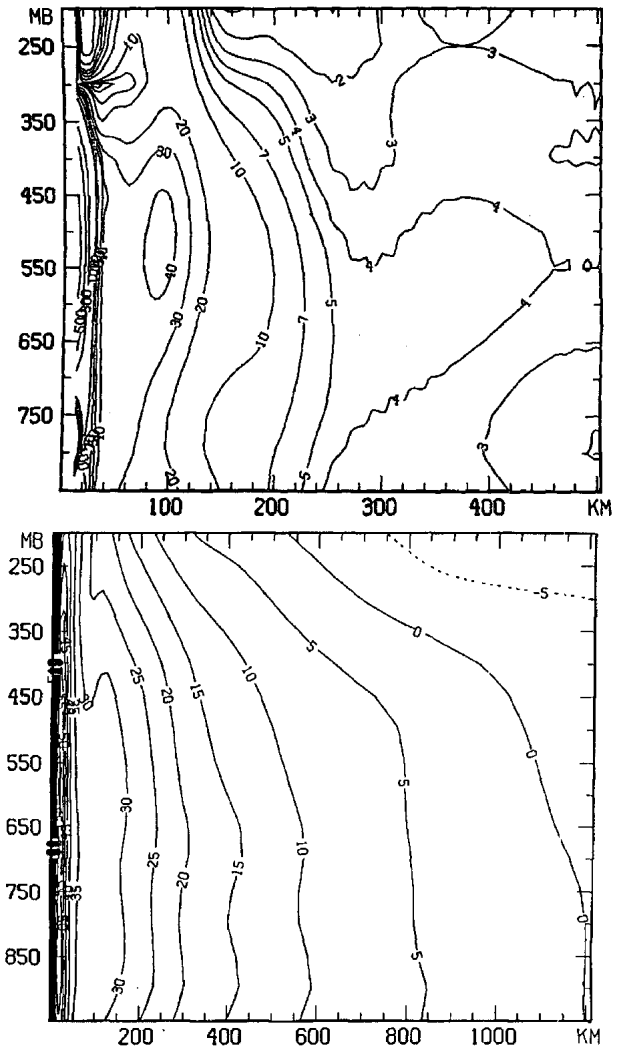

FIG. 2. Radial–height cross sections of Hurricane Gloria's (1985) azimuthal-mean (top) Rossby Ertel potential vorticity (10^{-7} m^2 s^{-1} K kg^{-1}) (Shapiro and Franklin 1995) and (bottom) tangential wind (m s^{-1}) (Franklin et al. 1993). Note the different horizontal scales in the top and bottom panels.

onstrated by Pearce (1993), who showed that for a steady-state axisymmetric vortex in gradient wind balance, the PV tendency equation in angular momentum coordinates (Thorpe 1985) reveals that the radial gradient of the frictional torque, $\partial(rF)/\partial r$, must vanish in the convective inflow region.

The nature of the inflow layer underneath a TC supports the many observational studies showing that the tangential winds in TCs approximately decrease similar to a modified Rankine vortex, although the decay exponent has been shown to vary. Many studies of mature storms were found to have decay exponent values between 0.5 and 0.7 (Hughes 1952; Malkus and Riehl 1960; Riehl 1963; Miller 1967; Sheets 1980; Anthes 1982; Franklin et al. 1993). Shapiro and Montgomery (1993), however, indicate that smaller values ($\alpha < 0.5$) are evident in the weaker storms studied by Riehl (1963) and Willoughby (1990a). This apparent variability was confirmed in the multistorm statistical studies of Gray and Shea (1973) and Samsury and Zipser (1995), where mean values found for α (0.5 and 0.4, respectively) were close to the expected theoretical value, but with relatively large standard deviations (0.3 and 0.2, respectively). It is believed that the stage of TC life cycle accounts for much of the variability in the tangential wind profile shape (e.g., Weatherford 1989). Many of the studies discussed, however, do not clearly specify the radial region used for the estimation of the modified Rankine decay exponent. Indeed, Petrova (1995) demonstrated that α increased for radial intervals farther away from the center of western North Pacific typhoons. This is in agreement with the large values evident at large radii in the composite Atlantic storm of Merrill (1984), as pointed out by Shapiro and Montgomery (1993).

The preceding discussion is based primarily on results from observational studies of low- and midlevel tangential winds obtained from aircraft missions into TCs of the Atlantic and North Pacific basins. Though scarce, observations at upper levels have indicated larger rates of tangential wind decay than at low and middle levels. The radial structure of tangential wind for Hurricane Gloria (Fig. 2a) illustrates this, in agreement with the results of Shea and Gray (1973) and Frank (1977, his Fig. 9). Nevertheless, the tangential wind decay in the near-core region for this particular case is still less than that of a pure Rankine vortex and, more importantly, the mean tropospheric layer primary circulation beyond the RMW likely possesses the approximate radial structure of a modified Rankine vortex.

d. Objectives of current work

Ideally, we would like to compare the radial PV structure of real TCs with idealized profiles. As already discussed, this is not currently practical or possible for a large number of storms. However, vertical relative vorticity may serve as a proxy for PV at single vertical levels, as in the recent flight-level observational study of the hurricane eye and eyewall region performed by Kossin and Eastin (2001). We follow suit in this study by comparing flight-level observations of tangential wind and relative vorticity, which are more widely available, with their equivalent idealized radial profiles.

Prior studies indicate that the modified Rankine vortex is a more realistic depiction of the tangential wind structure than pure Rankine vortices. The question remains as to how realistic are other ideal vortex profiles used in theoretical studies. In particular, how realistic are the family of vortices used in J95 and RMG that give contrasting results for the vortex in shear problem? How realistic is the rapid tangential wind decrease of the S90 vortex? Is the location of anticyclonic relative vorticity too close to the RMW? These particu-

lar vortex features, and the associated positive radial vorticity gradient, clearly differentiate the S90 vortex from the other idealizations shown in Fig. 1.

To our knowledge the current reexamination of the radial structure of TC primary circulation is one of the most comprehensive ever undertaken using flight-level observations. For reasons discussed earlier, we specifically focus on the *near-core* region between 1–3 RMW distances and apply the modified Rankine vortex in a consistent manner to estimate the radial TC structure. This particular vortex region has not been specifically emphasized in prior studies of the primary circulation. In one respect, we confirm the relative broadness observed in the radial structure of the tangential wind in the earlier studies discussed. What distinguishes this study, however, is the additional emphasis on the associated skirt of cyclonic relative vorticity observed in all TCs in the near-core region beyond the RMW. The current evidence of RMG and SM1,2 suggest that this region is of critical importance in supporting the resiliency of TCs subject to hostile vertically sheared environments. These important structural characteristics intrinsic to all TCs, are shown to be deficient in some analytical vortex profiles commonly used in theoretical studies of TC evolution. This study will thus, in effect, establish some "ground truth" for the idealization of radial structure of the TC primary circulation.

The paper is organized as follows. In section 2, the flight-level dataset is described. The methodology used for estimating the radial structure of the axisymmetric tangential wind and relative vorticity for both individual storms and multistorm composites is presented in section 3. For different TC intensity classes, section 4 compares the estimates of the radial structure of the primary circulation with idealized vortex profiles (Rankine, Rankine-with-skirt, Gaussian, and S90 vortices), whose analytical expressions for relative vorticity and tangential wind are given in appendix A. The implications for the vortex resiliency problem are discussed in section 5. In section 6, we summarize our findings and discuss future work.

2. Flight-level data

The data utilized for this study are extracted from the National Oceanic and Atmospheric Administration (NOAA) Hurricane Research Division (HRD) archive consisting of flight-level aircraft observations of Atlantic and eastern Pacific tropical cyclones between 1977 and 2001. During flight missions performed at standard pressure levels,[1] NOAA WP-3D and United States Air Force (USAF) WC-130 aircraft collect kinematic and thermodynamic measurements at the respective frequencies of 0.1 and 1.0 Hz. Radial "legs" of data are obtained as the aircraft perform repeated penetrations and exits of the TC core through the storm center. The radial legs of data are usually well distributed in the various storm quadrants, since they are typically obtained from one or more complete or partial "figure-four" flight patterns, most often in the N–S–E–W or NW–SE–NE–SW direction. Although the number of radial legs sampled and the duration of the flight mission may vary, the average flight mission typically lasts 6 h and results in eight radial legs of data.

The data processing for the HRD archive requires two key procedures. First, the original raw wind data is recomputed in a cylindrical-polar coordinate system moving with the cyclone center, in which the storm motion vector is subtracted from the wind velocity. The storm center location required for this coordinate transformation is estimated for each radial pass using the algorithm of Willoughby and Chelmow (1982), which was found to be accurate to within 3 km for intense hurricanes. Second, the resultant storm-relative data are smoothed and interpolated to a 300-point radial grid with nominal 0.5-km grid spacing using a Bartlett filter. Due to instrumentation failures and tape changes (Willoughby et al. 1982) the data bins are sometimes empty, resulting in gaps of missing data in radial flight legs. Further detailed discussion of aircraft instrumentation and data processing can be found in Jorgensen (1984), Willoughby et al. (1982), and Samsury and Zipser (1995).

The resulting HRD database (1977–2001), organized by storm and flight mission, is comprised of radial data arrays representing the kinematic and thermodynamic variables from the storm center to a maximum 150-km radial extent at 0.5-km intervals.[2] A total of 5124 radial legs of data were obtained from 644 missions into 72 storms during this period. The vast majority of flight missions occur between 900 and 600 mb, with the 700- and 850-mb levels sampled most often. Relatively few aircraft penetrations were performed at or above 500 mb.

Since the radial structure of the primary circulation is the focus of our study, the tangential component of the wind velocity is the only meteorological variable needed. Due to the precision of the modern inertial navigation (INE) system, greatly improved over the Doppler aircraft navigation used prior to the mid-1970s (Willoughby 1990b), the raw horizontal wind measurements are accurate to within 1.0 and 2.0 m s^{-1} for the NOAA WP-3D and USAF WC-130 aircraft, respectively (OFCM 1993; Kossin and Eastin 2001). However, additional error is likely introduced into the storm-

[1] Most flight missions were performed at the standard pressure levels of 900, 850, 700, 600, 500, and 400 mb. A few flight missions, however, were undertaken at 950, 800, 750, 650, and 550 mb.

[2] There exist several flight missions where the maximum radial extent of the data is either 300 km (Arthur 1984; Gloria 1985) or 75 km (Emily 1987). Since the number of data points in the radial array is fixed (300) in the HRD database, the nominal 0.5-km grid spacing is effectively doubled (1.0 km) or halved (0.25 km).

relative winds due to the uncertainty in the storm center location (Samsury and Zipser 1995).

3. Methodology

The HRD flight-level data archive is well suited for investigating the axisymmetric TC structure (Willoughby and Rahn 2004). For individual flight missions, the procedure for estimating the azimuthal-mean radial structure of tangential wind and relative vorticity is first discussed. These azimuthal-mean estimates for individual storm cases are then utilized to construct a multistorm composite representation of the axisymmetric vortex structure. Both methods enable comparison with idealized vortex profiles that have been used to represent the axisymmetric primary circulation in theoretical studies.

a. Individual storm estimates of the axisymmetric primary circulation

The procedure described here involves the estimation of the radial distribution of the azimuthal-mean tangential velocity by utilizing the available radial legs of data obtained during a single flight mission. From this estimate, the azimuthal-mean relative vorticity is easily derived. Despite the limited azimuthal resolution of the flight-level data, the persistence that is commonly observed in the radial structure of the tangential velocity from profile to profile enables a reasonably accurate estimate of the slowly evolving axisymmetric component. This persistence is demonstrated by tangential wind asymmetry estimates.

1) TANGENTIAL VELOCITY

In previous flight-level studies, linear least squares fits to the time-dependent data allowed the estimation of the axisymmetric tangential wind and geopotential height evolution during the time period of the data sampling (Willoughby et al. 1982; Willoughby 1990a,b). Only a "snapshot" of the axisymmetric tangential wind, however, is desired here. An azimuthal-mean estimate is obtained from N radial legs using an arithmetic mean at each radius r_i,

$$\overline{V}_i = \frac{1}{N}\sum_{j=1}^{N} V_{ij}, \tag{1}$$

with the subscripts i, j denoting the radial and azimuthal bin locations, respectively. The estimated azimuthal-mean radial profiles of tangential wind are then smoothed with a 5-km (nine point) Bartlett filter for the desired effect of reducing transient peaks and removing the smallest scale filamentary structure. The resultant $\overline{V}$ profile estimate is representative of the axisymmetric component at the midpoint time of the sampling period and is in close agreement with estimates obtained using the least squares methods of Willoughby et al. (1982).

The averaging procedure often requires the choice of an optimal subset of the available radial legs that maximizes the radial extent of the azimuthal-mean estimate both within and outside the RMW, while retaining uniformity in the radial leg distribution. The removal of some radial legs from the averaging process is often necessary when the radial extent of the flight leg data is limited or large gaps (>10 km) are present, since their inclusion in the averaging procedure would result in a truncated or discontinuous azimuthal-mean radial profile. Approximately 80% of the flight missions qualify for the azimuthal-averaging procedure, resulting in 526 estimated azimuthal-mean radial profiles of tangential wind and relative vorticity. The flight missions in which data were absent in one or more storm quadrants did not qualify for azimuthal averaging. This situation is often a consequence of the prohibition from flying over land for an approaching storm, in which the data sampling is limited in the storm quadrants nearest landfall (Willoughby 1990a).

2) RELATIVE VORTICITY

The radial profiles of azimuthal-mean relative vertical vorticity are most easily estimated from the smoothed azimuthal-mean tangential wind profiles ($\overline{V}$) described above. The symmetric vertical component of relative vorticity $\overline{\zeta}$ is related to the symmetric tangential wind $\overline{V}$ by the equation $\zeta(r) = \overline{V}/r + d\overline{V}/dr$. The shear term in the relative vorticity is approximated by centered differencing, resulting in $\overline{\zeta}(r_i) = \overline{V}_i/r_i + (\overline{V}_{i+1} - \overline{V}_{i-1})/(r_{i+1} - r_{i-1})$.

3) ASYMMETRY

To supplement the axisymmetric radial TC structure we additionally provide estimates of the asymmetry in the tangential wind field. This enables an assessment of the accuracy of our azimuthal-mean estimate and demonstrates the degree of persistence exhibited by the tangential wind data in the various storm quadrants. Here, the magnitude of the total asymmetry at each radius, V_i', is estimated from the rms deviation from the azimuthal-mean tangential wind $\overline{V}$ and is given by

$$V_i' = \frac{1}{N}\sqrt{\sum_{j=1}^{N} (V_{ij} - \overline{V}_j)^2}. \tag{2}$$

Note that this estimate of the tangential wind asymmetry magnitude may have contributions that arise from both the evolution of the axisymmetric component during the sampling time period and the error induced by the imprecise determination of the TC center.

4) AN ILLUSTRATIVE EXAMPLE

An example of the procedure employed here is discussed for a particular flight mission into Hurricane Floyd (1999). The radial profiles of tangential wind and associated individual radial legs are displayed in Fig. 3,

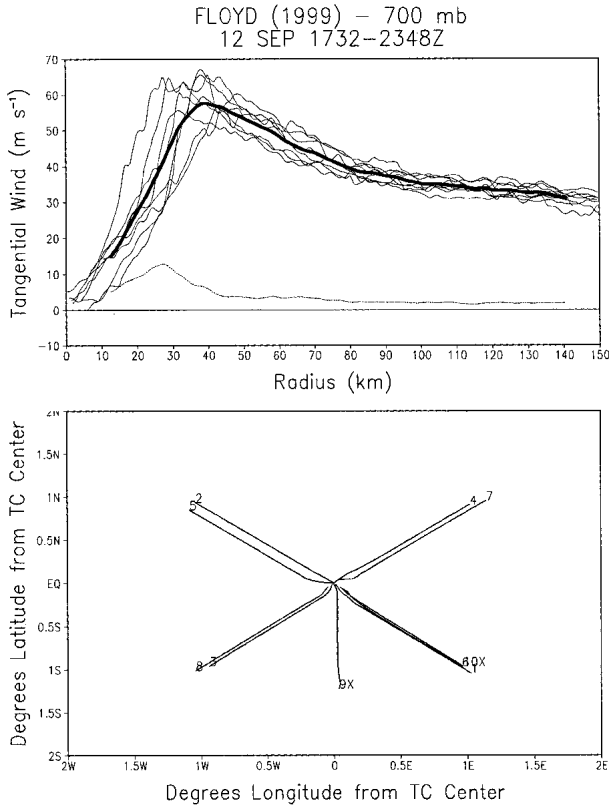

FIG. 3. (bottom) Radial flight leg segments, numbered in the order of data sampling, are plotted relative to the center of Hurricane Floyd (1999). Here, X denotes exclusion of the indicated radial leg from azimuthal averaging. (top) Radial leg profiles of tangential velocity (thin curves) overlaid with the azimuthal-mean estimate $\overline{V}$ (thick curve) representing the midpoint time of the flight mission. The magnitude of the total asymmetry V' is estimated by the rms deviation from the azimuthal-mean tangential velocity $\overline{V}$ (dotted curve).

in addition to estimates of the azimuthal-mean ($\overline{V}$) and magnitude of the total asymmetry (V'). The choice of the first 8 of the 10 available radial legs of data sampled was sufficient for obtaining reasonable $\overline{V}$ estimates extending from approximately 10–140-km radius. The particular case chosen here exhibited a large variation in the radius of the local tangential wind maxima associated with the individual radial legs. This is reflected in the maximum of V' inside the azimuthal-mean RMW, which may arise from a combination of real core asymmetries, symmetric vortex contraction associated with intensification (or expansion) during the sampling period, or from error in the storm center determination. Since Floyd was rapidly intensifying during this particular flight mission (Mallen 2004), all three factors likely contributed to the peak in V'. Outside the RMW, the relatively small and approximately constant values of V' are indicative of the slow coherent decay of tangential wind in all storm quadrants. Overall, the degree of asymmetry is small and the azimuthal-mean estimate $\overline{V}$ in Fig. 3 is representative of the axisymmetric structure of Floyd at the midpoint time of the flight mission. The structural features of Floyd discussed here were also observed in the storms studied by Willoughby et al. (1982) and, as discussed in section 4c, are persistent in TCs.

b. Multistorm composites of the primary circulation

Multistorm composite approaches in some previous flight-level studies of the mean tangential wind field have utilized a method that combines all of the individual radial legs from one or more storms by averaging with respect to radial distance from the *local* radius of maximum wind. By aligning the peaks of the individual radial legs, this approach has the advantage of separating profile features inside and outside of the RMW (Shea and Gray 1973), and has proven useful for understanding eye–eyewall dynamics (Kossin and Eastin 2001) and secondary maxima associated with outer convective bands (Samsury and Zipser 1995). This averaging method, however, is not appropriate for estimating the axisymmetric TC structure. According to Willoughby (1991), an overestimated supergradient maximum is produced in which the often sharply peaked transient local maxima of the individual radial leg profiles are preserved.

A novel composite method is introduced here to obtain the average normalized radial structure of tangential wind and relative vorticity from a group of individual storm cases represented by their $\overline{V}$ and $\overline{\zeta}$ radial profile estimates. As discussed previously, the estimated azimuthal-mean $\overline{V}$ profiles for individual storm flight missions are first obtained by appropriately averaging the individual radial legs at fixed radii [Eq. (1)], thereby enabling the proper estimation of the *axisymmetric tangential wind maximum* ($\overline{V}_{\max}$) and the corresponding RMW. The radial profiles of $\overline{V}$ for each storm case are then scaled so that the resultant profile possesses a unit maximum located at unit radius. A nondimensional composite tangential wind may then be obtained by averaging[3] together the normalized azimuthal-mean estimates ($\overline{V}/\overline{V}_{\max}$) with respect to a normalized radius (r/RMW). To assess the mean asymmetry in the tangential wind field for a group of storm cases, this method is also applied to the radial profiles of V'. The only difference in estimating the composite structure for the azimuthal-mean relative vorticity is the normalization of the radial profiles of $\overline{\zeta}$ by the value at the RMW, $\overline{\zeta}_{\max} = \overline{V}_{\max}/\text{RMW}$, which is consistent with the scaling used to normalize $\overline{V}$.

[3] Since the constant radial grid spacing (Δr = 0.5 km) of the flight-level data will vary from case to case after radial scaling by the differing RMW ($\Delta r' = \Delta r/\text{RMW}$), the normalized data are interpolated to a common nondimensional radial grid for the purpose of composite averaging. To preserve the data resolution of all the individual cases, the common grid spacing associated with the case possessing the largest RMW is chosen ($\Delta r'_{\min} = \Delta r/\text{RMW}_{\max}$).

Normalizing the estimated radial profiles of azimuthal-mean tangential velocity ($\overline{V}$) and relative vorticity ($\overline{\zeta}$) prior to composite averaging clearly facilitates comparison with idealized vortex profiles, which are often expressed in nondimensional form (appendix A). For a sample of major hurricane cases, Fig. 4 illustrates how the normalization preserves the underlying profile shape in the mean composite radial structure. Note the uniformity in the radial profile shape for the majority of cases.

4. Results

a. Vortex parameter relationships

The necessary data requirements for estimating the radial structure of the axisymmetric primary circulation for individual storm flight missions (section 3a) yield 526 estimated radial profiles of azimuthal-mean tangential wind $\overline{V}$ and relative vorticity $\overline{\zeta}$. The distribution of these cases, represented by the basic scales, RMW and $\overline{V}_{\max}$, is depicted in Fig. 5. The distribution of $\overline{V}_{\max}$ spans all TC intensity classifications from tropical depressions to category 5 hurricanes, and is believed to be fairly representative of TCs (Willoughby and Rahn 2004). The range in RMW is large, from 8.5 to 178 km.

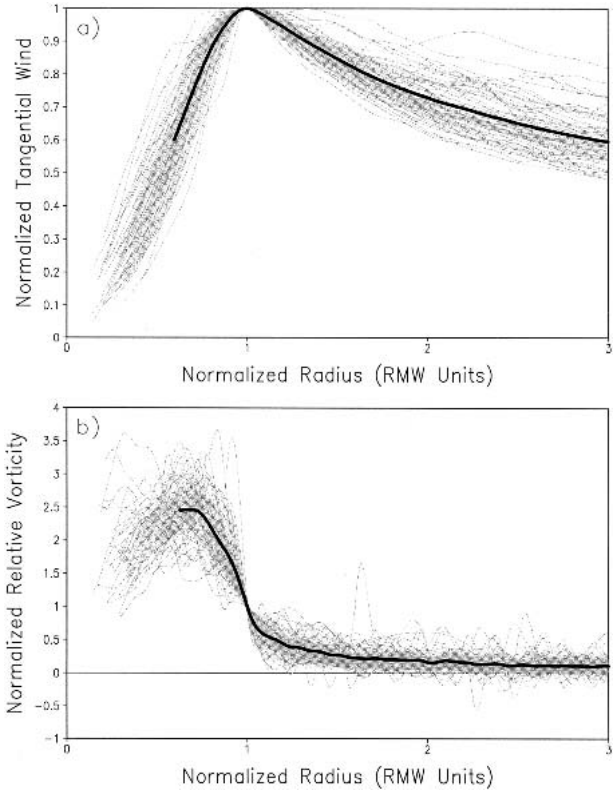

FIG. 4. Normalized radial profiles of azimuthal-mean (a) tangential wind $\overline{V}$ and (b) relative vorticity $\overline{\zeta}$ estimated from 72 flight missions into major hurricanes (thin gray curves) overlaid with the mean composite profile (solid black curve).

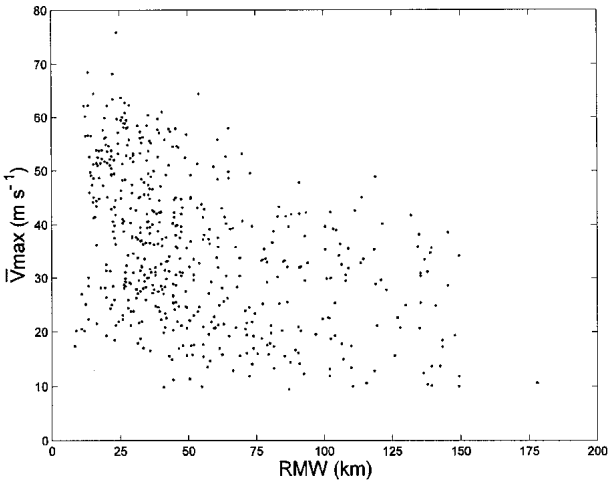

FIG. 5. A scatterplot depicting the relationship between the maximum azimuthal-mean tangential velocity ($\overline{V}_{\max}$) and the RMW obtained from the estimated radial profiles of azimuthal-mean tangential velocity $\overline{V}$ representing the 526 storm cases.

Note, however, that the 150-km radial constraint may preclude the observation of the true $\overline{V}_{\max}$ in some cases. Figure 5 indicates essentially no statistical relationship between the RMW and $\overline{V}_{\max}$ except for the most intense storms, where the wind maximum tends to be located close to the TC center, consistent with the results of Shea and Gray (1973).

For this study, we are primarily interested in the radial structure of the primary circulation between 1–3 RMW distances, the region believed to contain the critical radius for a simple tilt mode (see section 1b). This entire radial range, however, can be investigated only for the cases where the RMW is within 50 km of the TC center. The greatest density of storm cases is located here (Fig. 5) and represents 60% (316) of the available radial profile estimates of $\overline{V}$ and $\overline{\zeta}$. The three-RMW constraint further limits the sample to 251 cases. The 275 cases excluded here, most of which possess RMW $>$ 50 km, are represented by radial profiles of $\overline{V}$ and $\overline{\zeta}$ whose maximum radial extent is less than three RMW distances from the TC center. We point out in advance that although these cases are limited in outward extent, their radial structure does not appear to deviate from the results found in the following analysis.

To characterize the primary circulation beyond the RMW, the modified Rankine decay exponent α is calculated for all 251 estimated radial profiles of azimuthal-mean tangential wind $\overline{V}$. This is one possible way to further specify the axisymmetric radial structure, in addition to the RMW and $\overline{V}_{\max}$. Values of α are determined from $\overline{V}$ at two specified radii using the following relationship derived from (A1):

$$\frac{\overline{V}_1}{\overline{V}_2} = \left(\frac{r_2}{r_1}\right)^{\alpha}. \tag{3}$$

In this analysis, $\overline{V}$ is specified at one and three RMW distances from the TC center.

To obtain a meaningful stratification of the cases, the relationships between α and both $\overline{V}_{\max}$ and RMW are investigated. Despite large scatter in the relationship, Fig. 6 reveals a tendency for increasing values of α for increasing $\overline{V}_{\max}$. This is consistent with the sharpening of the wind profile that has been observed after periods of intensification (Willoughby et al. 1982; Willoughby 1990a). No statistical correlation, however, is found between α and RMW (not shown).

b. Observed versus idealized vortex profiles

In order to efficiently compare the large number of storm cases to the idealized vortices, it is desirable to construct nondimensional composite radial profiles of azimuthal-mean tangential wind and relative vorticity from the respective $\overline{V}$ and $\overline{\zeta}$ estimates, using the method described in section 3b. Since the radial structure outside the RMW exhibits some dependence on the vortex intensity (Fig. 6), the individual storm cases are first stratified by $\overline{V}_{\max}$. The values that define the three categories are somewhat arbitrary, and approximately represent the common characterization of *prehurricane* (<30 m s^{-1}), *minimal hurricane* (30–50 m s^{-1}), and *major hurricane* (>50 m s^{-1}) categories, which are otherwise commonly defined in terms of maximum sustained surface wind speeds. The total number of cases for each TC intensity class and their distribution among the various flight levels is displayed in Table 1. Note that flight missions typically occur at higher altitudes for increasingly intense storms, a consequence of the danger in flying at lower levels (Willoughby and Rahn 2004).

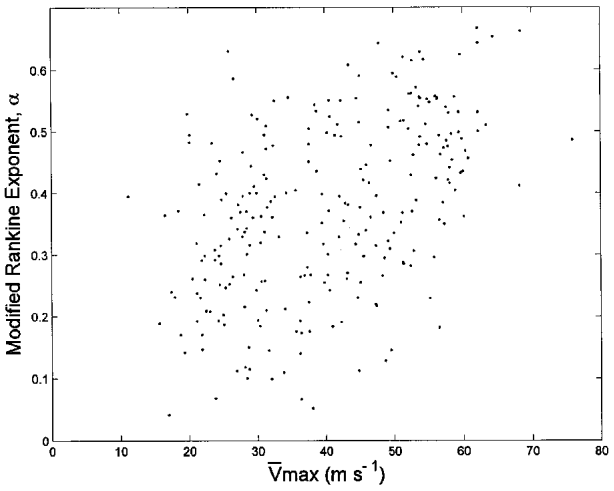

FIG. 6. A scatterplot depicting the relationship between the maximum azimuthal-mean tangential velocity ($\overline{V}_{\max}$) and the equivalent modified Rankine vortex decay exponent (α) associated with 251 storm cases. The decay exponent α is calculated from the radial profile estimates of azimuthal-mean tangential velocity $\overline{V}$ between 1 and 3 RMW distances.

TABLE 1. Tropical cyclone intensity classes. Number of flight missions at specified pressure levels for three intensity classes: major hurricane (>50 m s^{-1}), minimal hurricane (30–50 m s^{-1}), and prehurricane (<30 m s^{-1}). The estimated azimuthal-mean radial profiles of tangential velocity $\overline{V}$ (and relative vorticity $\overline{\zeta}$) associated with each flight mission satisfy the minimum data requirement of three RMW distances.

	Prehurricane storms	Minimal hurricane	Major hurricane	All TCs
900–950 mb	24	4	1	29
800–850 mb	40	41	7	88
700–750 mb	7	56	52	115
600–650 mb	2	2	10	14
500–550 mb	0	3	2	5
Total	73	106	72	251

For each TC intensity class, the nondimensional composite radial structure of tangential wind and relative vorticity, in conjunction with their equivalent modified Rankine vortex profiles, are compared with pure Rankine, Gaussian, and S90 idealized vortex profiles. The average and extremes of vortex structure represented by three individual cases (one from each intensity class), in terms of the rate of tangential wind decay outside the RMW (α), are also presented and compared to the ideal vortices.

To complement the composite and individual storm profiles, statistics are computed for the distribution of α and summarized in Table 2. Before discussing results for each intensity class, note that our mean estimate of α for the entire sample, calculated from radial profiles of *azimuthal-mean* tangential wind, agrees closely with prior multistorm flight-level studies that, in contrast, estimated α from many individual radial leg profiles (see section 1c). The lower standard deviation of α (Table 2) found here, however, is believed to be a consequence of the suppression of variability resulting from azimuthal averaging.

1) PREHURRICANE STORMS

A composite radial profile of azimuthal-mean tangential wind and relative vorticity from all 73 prehurricane cases are shown in Fig. 7 and compared with the idealized vortex profiles. Note that a comparison of composites (not shown) for the 850- and 900-mb sub-

TABLE 2. Modified Rankine vortex statistics. For the three TC intensity classes defined in Table 1, statistics are computed for the decay exponent (α) of the equivalent modified Rankine vortex associated with the individual storm cases. The decay exponent α is calculated for each radial profile of azimuthal-mean tangential wind $\overline{V}$ between 1 and 3 RMW distances [Eq. (2)].

Category	Mean α	Std dev α	Range α
Prehurricane	0.31	0.12	0.04–0.63
Minimal hurricane	0.35	0.14	0.05–0.64
Major hurricane	0.48	0.11	0.18–0.67
All TCs	0.37	0.14	0.04–0.67

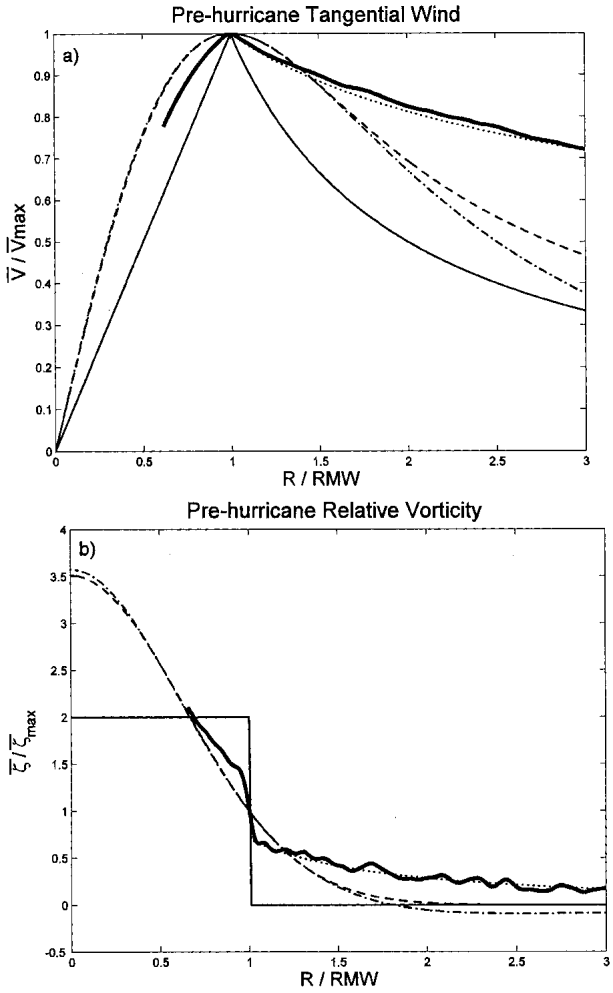

FIG. 7. Composite normalized radial profiles of azimuthal-mean prehurricane (a) tangential velocity and (b) relative vorticity (thick solid line) compared with equivalent idealized radial profiles for Rankine (thin solid line), Gaussian (dashed line), and S90 (dash–dot line) vortices, in addition to the best-fit modified Rankine (dotted line) vortex ($\alpha = 0.31$).

sets (Table 1), where most prehurricane flight missions occur, revealed essentially no difference in the nondimensional radial structure.

Within and near the RMW, the composite prehurricane tangential wind profile shape is broader than the sharply peaked Rankine vortex profile but not quite as broad as a Gaussian vortex (Fig. 7). This corresponds to the larger than Gaussian, yet finite, gradient of relative vorticity across the RMW. In the neighborhood of the RMW, the rate of tangential wind decrease is much less than the rapid decay of a pure Rankine vortex but is greater than the broadly peaked Gaussian and S90 vortices. Although the corresponding relative vorticity is slightly lower than Gaussian values just beyond the RMW, it is appreciably nonzero, in contrast to the characteristic zero relative vorticity of a Rankine vortex.

Most pertinent for this study, however, is the region farther outward from the wind maximum between roughly 1.5 and 3 RMW distances from the center. Here, the composite prehurricane tangential wind, similar to the equivalent modified Rankine vortex ($\alpha = 0.30$), decreases more slowly with distance than the Gaussian vortex and therefore slower than all other idealizations. This naturally corresponds to the slower monotonic decrease in relative vorticity, and thus overall greater values of relative vorticity for the composite prehurricane in this region. This is in sharp contrast to the rest of the ideal vortices, whose exaggerated tangential wind decrease results in negligible (Gaussian), zero (Rankine), or even negative (S90 vortex) relative vorticity. Clearly, the idealized vortices discussed here are highly unrealistic in representing the composite prehurricane structure in the near-core region outside of the RMW.

The range in the rate of tangential wind decay for prehurricane storms is indicated by the large variability in α (Table 2, Fig. 6). A surprising number of prehurricane cases possess large values of α, a characteristic typically ascribed to the more sharply peaked wind maxima of more developed hurricanes. However, due to the large number of storm cases possessing relatively flat-shaped wind profiles, the broadness in the radial structure of the composite prehurricane storm presented here is consistent with previous characterizations of the primary circulation of weak TCs (Willoughby 1990a; Weatherford 1989).

As an example of very broad TC structure, consider Atlantic Tropical Storm Fran in its early stage of development on 30 August 1996. The radial profiles of azimuthal-mean tangential wind $\overline{V}$ and relative vorticity $\overline{\zeta}$ (Fig. 8) resemble the Gaussian vortex from within and just outside the RMW located at 24 km. The radial structure of Fran, however, diverges dramatically from all of the idealized vortices beyond approximately 30 km as $\overline{V}$ decreases very slowly to 70–75 km (~3 RMWs), with an approximate decay exponent value of $\alpha = 0.15$. The large-scale trend in $\overline{\zeta}$, despite the small-scale fluctuations (on the order of 5–10 km), is decidedly monotonic decreasing with significantly larger values than all of the idealized vortices. Comparison of Fran's radial structure with its equivalent modified Rankine vortex ($\alpha = 0.15$) elucidates the appreciable negative radial gradient of the underlying relative vorticity. This supports our contention that the broadness of the radial profile of tangential wind and the corresponding significant skirt of relative vorticity beyond the RMW distinguishes real prehurricane structure from some of the unrealistic idealizations commonly used in studies of TC evolution.

2) MINIMAL HURRICANES

The majority of storm cases are classified as minimal hurricanes (see Table 1). Their estimated $\overline{V}$ and $\overline{\zeta}$ profiles are then averaged, as previously done for the pre-

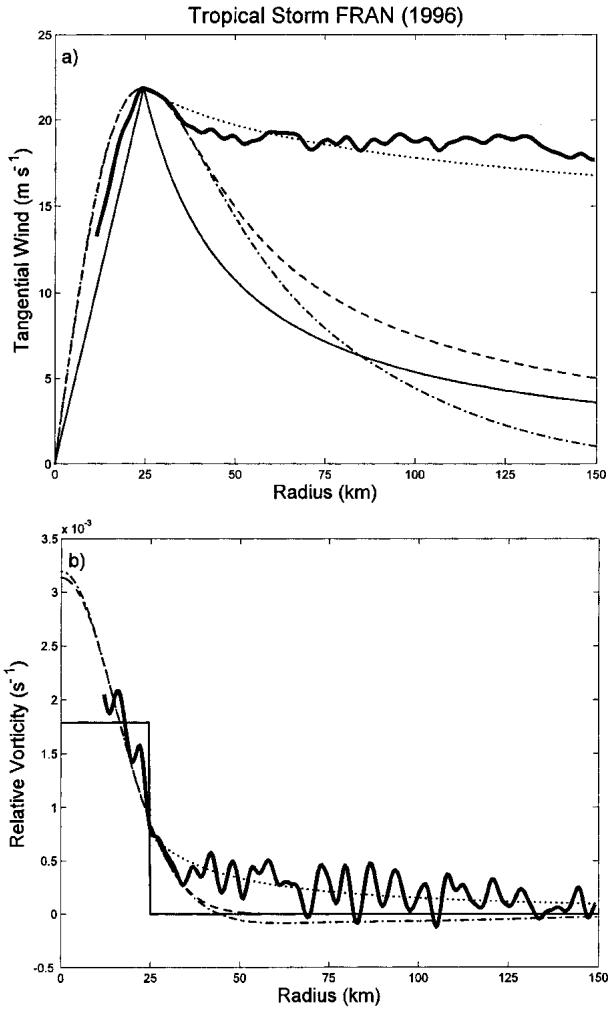

FIG. 8. Azimuthal-mean radial profile of (a) tangential velocity $\overline{V}$ and (b) relative vorticity $\overline{\zeta}$ estimated from observations of Tropical Storm Fran during the period 0506–1243 UTC 30 Aug 1996 (solid line), overlaid with their equivalent modified Rankine vortex profile (dotted line, $\alpha = 0.15$) and compared with equivalent idealized Rankine (thin solid line), Gaussian (dashed line), and S90 (dash–dot line) ideal vortices.

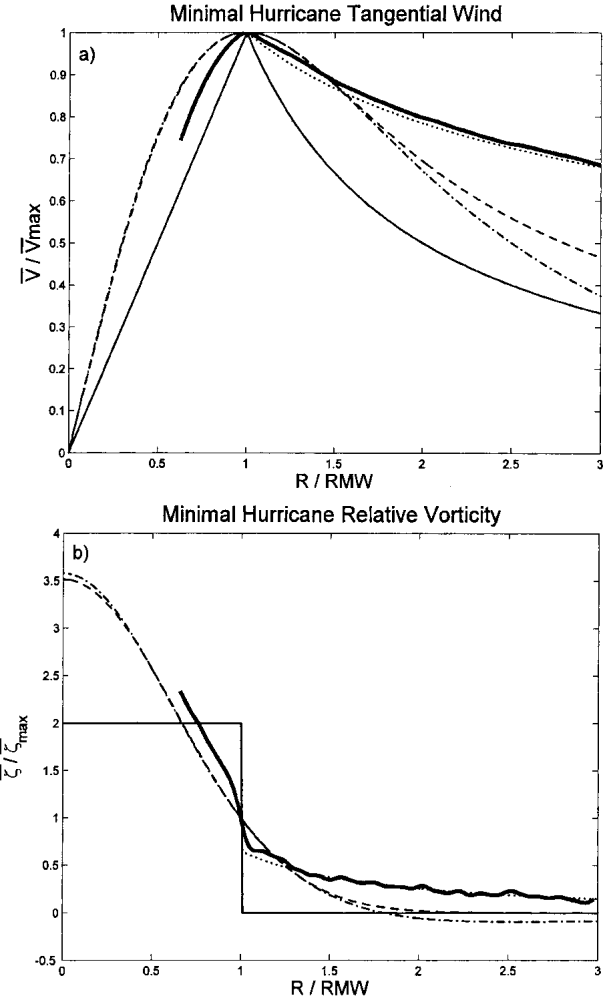

FIG. 9. Same as in Fig. 7 except for minimal hurricanes ($\alpha = 0.35$).

hurricane group. Again, no difference in the composite radial structure of tangential wind and relative vorticity is observed between the 850- and 700-mb levels (not shown), which comprised more than 90% of the minimal hurricane cases.

Similar to the prehurricane class, the composite axisymmetric tangential wind profile shape within roughly 1.5 RMW is broader than a pure Rankine vortex, yet narrower than the equivalent Gaussian vortex (Fig. 9). This is again manifested in the sharper than Gaussian decrease of relative vorticity across the RMW yet slower than the discontinuous jump from constant to zero vorticity that is characteristic of Rankine vortices. As a consequence, significant cyclonic azimuthal-mean relative vorticity exist outside the RMW. The composite minimal hurricane structure beyond 1.5 RMW distances is quite different than the ideal vortices, as in the prehurricane group. The fractional decrease of tangential wind with distance is greater for the composite minimal hurricane than the composite prehurricane storm, resulting in a larger decay exponent for the equivalent modified Rankine vortex ($\alpha = 0.35$). In contrast to the idealized vortices, however, the comparably slow composite tangential wind and relative vorticity decrease results in the conspicuous broadness of their radial profile shape in the near-core region outside the RMW.

The minimal hurricane intensity classification exhibits the largest variability in vortex structure, in terms of the standard deviation of the modified Rankine decay exponent (Table 2). This is likely a consequence of a secondary concentration in the modified Rankine decay exponent near $\alpha = 0.5$ (Fig. 6), the theoretical value expected for mature steady-state hurricanes (Pearce 1993; Emanuel 1986). However, the majority of cases

here still exhibit relatively slow tangential wind decay, as indicated by both the mean value ($\alpha = 0.35$) and the composite minimal hurricane structure (Fig. 9).

Category 2 storm Bonnie on 23 August 1998 is a representative case of the minimal hurricane class and can be considered an average case for the entire sample in terms of the rate of tangential wind decrease in the near-core region outside the RMW (see Table 2). The radial structure of Bonnie (Fig. 10) is very similar to the composite minimal hurricane in all aspects, except that the small-scale fluctuations in $\bar{\zeta}$ beyond the RMW slightly obscure the monotonically decreasing trend that is more clearly evident in the composite relative vorticity (Fig. 9b). The slow underlying monotonic decrease of azimuthal-mean relative vorticity, which can be represented by the $r^{-(\alpha+1)}$ decay of the equivalent modified Rankine relative vorticity ($\alpha = 0.35$), ensures appreciable cyclonic relative vorticity (and negative radial gradients) out to large radii.

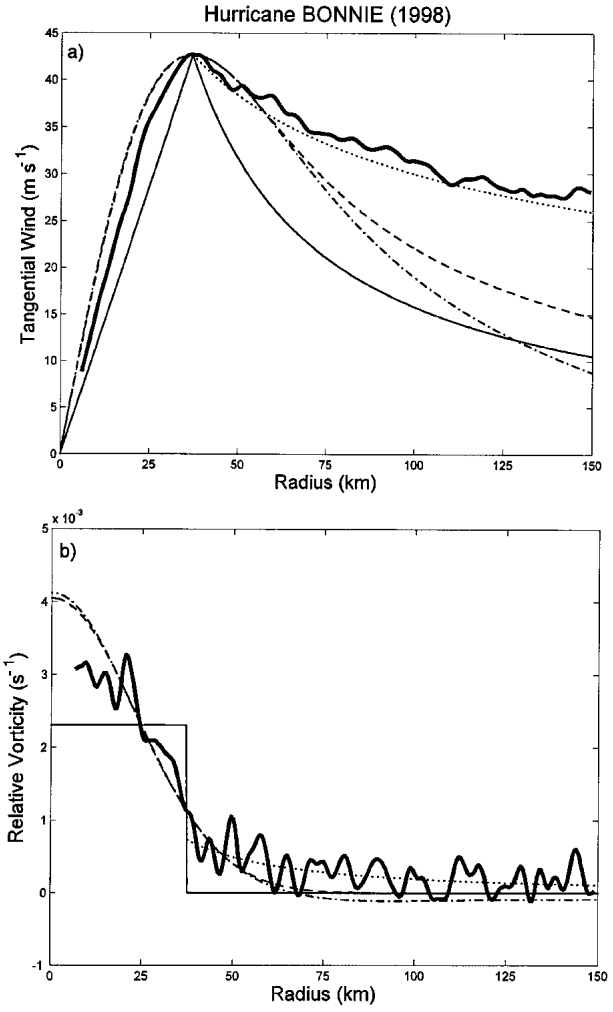

FIG. 10. Same as in Fig. 8 except for Hurricane Bonnie during the period 0257–0538 UTC 23 Aug 1998 and $\alpha = 0.35$.

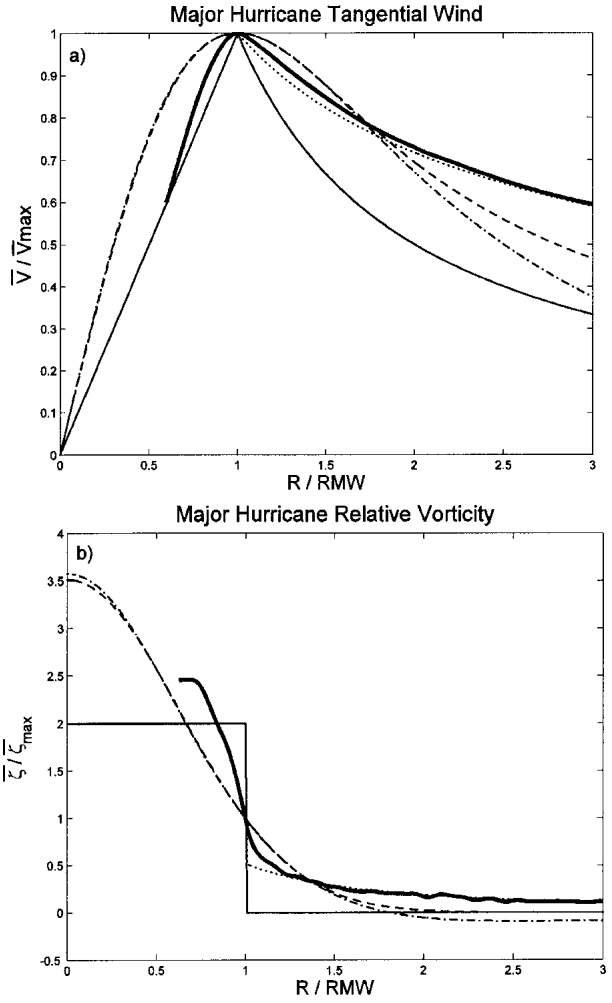

FIG. 11. Same as in Fig. 7 except for major hurricanes ($\alpha = 0.48$).

3) MAJOR HURRICANES

This class of TCs discussed here represents the most intense storms in this study, of which the vast majority of flight missions occur at 700 mb (Table 1). Inside the RMW, the radial profile of the composite major hurricane vortex (Fig. 11, also see Fig. 4) appears quite different than the composite structure of the prehurricane and minimal hurricane classes. The major hurricane group has much less Gaussian vorticity characteristics in this region than the other two classes (Figs. 7b, 9b), which can be clearly seen in the departure from Gaussian relative vorticity (Fig. 11b). The very rapid increase in tangential wind speed, far from the linear increase of a Rankine vortex, results in a relative vorticity maximum between the center and the RMW (also see Fig. 4b). The latter arises in association with the strong vortex-tube stretching of vertical vorticity by the convective and mesoscale updrafts within the hurricane eyewall (Schubert et al. 1999). This type of tangential

wind structure is expected to support a combined barotropic–baroclinic (shear) instability and related eyewall mesovortex phenomenology (Schubert et al. 1999; Montgomery et al. 2002; Nolan and Montgomery 2002; Kossin and Schubert 2001). Such interior vorticity redistribution processes typically evolve on a smaller (radial shear) time scale than the tilted vortex response (scale separation) and hence should not significantly alter the tilted vortex predictions using the monotonic PV distributions summarized in the introduction. For the remaining discussion we will assume that this is the case.

Outside the RMW, the radial structure of the composite major hurricane vortex is qualitatively similar to the prehurricane and minimal hurricane classes. However, the mean fractional decrease of tangential wind is much greater than both the mean prehurricane and minimal hurricane vortex, as evidenced by the larger decay exponent of the equivalent modified Rankine vortex ($\alpha = 0.47$). Nevertheless, the faster tangential wind decay of major hurricanes is still relatively slow enough to allow for significant cyclonic relative vorticity (and radial gradients) in comparison to the idealized vortices in the 1–3 RMW radial region.

The major hurricane class appears to largely exhibit characteristics that agree with theoretical predictions for mature steady-state hurricanes, in which the decay exponent values are highly concentrated near $\alpha = 0.5$ (Fig. 6). Despite possessing the lowest standard deviation of the intensity classes, the range of α for major hurricanes is still rather large due to a few outliers. The two lowest values of α are, in fact, associated with cases possessing pronounced secondary tangential wind maxima (Andrew 1992, Floyd 1999) between 1–3 RMW distances, most likely associated with concentric eyewalls.

The storm case exhibiting the most extreme tangential wind decrease in the entire dataset belongs to this category of hurricane intensity. During the period 1854–2053 UTC on 13 September 1988, Hurricane Gilbert (Fig. 12) was near its peak intensity of 888 mb with a value of $\overline{V}_{\max}$ close to 70 m s^{-1}. The large decrease in $\overline{V}$ beyond the RMW resulted in a decay exponent of $\alpha = 0.67$, according to the best-fit modified Rankine vortex between 1–3 RMW distances. The trend of $\overline{\zeta}$ in this region, though only slightly obscured by the smaller-scale fluctuations, is monotonically decreasing (Fig. 12b). Even in this most extreme case (largest α) the important cyclonic skirt evident in $\overline{\zeta}$ beyond the RMW is still significantly greater than for equivalent Rankine, Gaussian, and S90 ideal vortices.

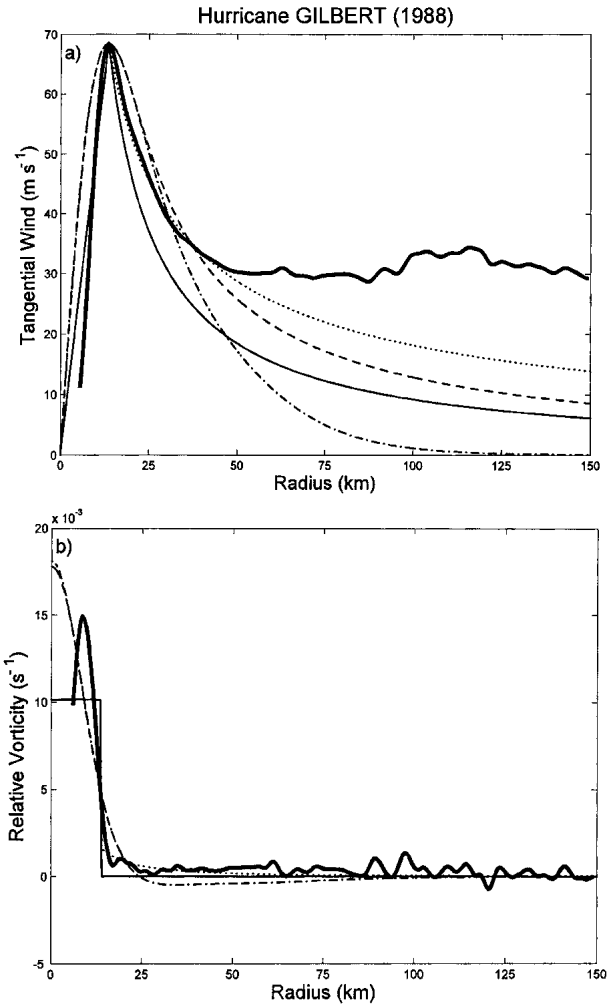

FIG. 12. Same as in Fig. 8, except for Hurricane Gilbert during the period 1854–2053 UTC 13 Sep 1988 and $\alpha = 0.67$.

c. Estimates of vortex asymmetry

The results thus far have demonstrated that the radial structure of the axisymmetric primary TC circulation in the near-core region beyond the RMW is characterized by a relatively slow decay of tangential wind in association with a broad cyclonic skirt of relative vorticity. By assessing the degree of asymmetry in the tangential wind field here, we demonstrate that the broadness observed in the primary circulation is representative of the radial structure in the various storm quadrants.

To facilitate this discussion, the normalized composite radial profiles of azimuthal-mean tangential wind for the three TC intensity classes, in addition to the corresponding composite asymmetry estimates, are overlaid in Fig. 13. A well-known property of developing TCs is depicted, in which the radial profile of the azimuthal-mean tangential wind becomes more sharply peaked (larger α) as the asymmetry decreases. This larger rate of tangential wind decay and higher degree of circular symmetry was previously noted by Croxford and Barnes (2002). The maximum of the composite asymmetry estimate is located within the RMW and is less than 20% of $\overline{V}_{\max}$ for all intensity classes. This peak in the tangential wind variance, discussed in sec-

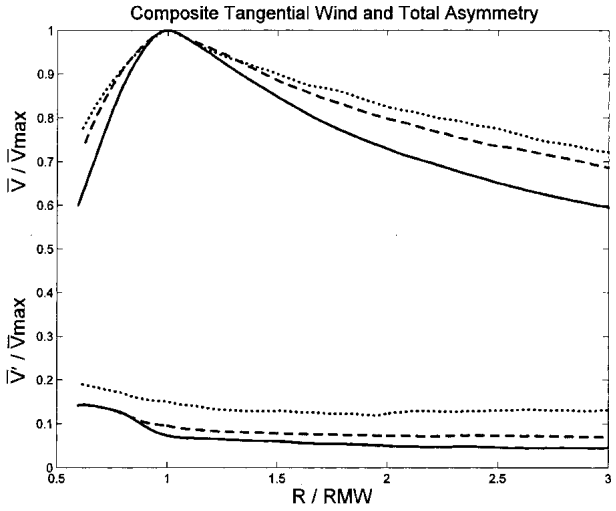

FIG. 13. Composite radial profiles of the normalized azimuthal-mean tangential wind $\overline{V}$ and corresponding tangential wind asymmetry V' for the major hurricane (solid), minimal hurricane (dashed), and prehurricane (dotted) intensity classes (see Tables 1, 2).

tion 3a for the specific case of Hurricane Floyd (Fig. 3), is apparently a persistent feature of the flight-level dataset. In the near-core region outside the RMW, the composite asymmetry estimate gradually decreases to nearly constant values: less than 5% of $\overline{V}_{\max}$ for the major hurricane class and slightly greater than 10% for prehurricane storms (Fig. 13).

The characteristics of the composite radial structure of the total asymmetry are also representative of the majority of individual storm cases. In particular, the low and approximately constant asymmetry estimates in the near-core region outside the RMW indicate that the azimuthal variation in the tangential wind field is small. The relatively slow rate of tangential wind decay observed in the azimuthal-mean radial structure is thus expected to persist in the different storm quadrants of TCs. This is consistent with previous flight-level studies (e.g., Gray and Shea 1973; Samsury and Zipser 1995; see section 1c) that found slower than Rankine tangential wind decay in the individual radial leg profiles representing various storm quadrants.

d. Influence of secondary tangential wind maxima

An important issue concerning the broadness observed in the primary circulation is the contribution of secondary tangential wind maxima that are sometimes present outside the RMW. To distinguish the secondary maxima associated with mesoscale phenomena from smaller-scale profile features, Samsury and Zipser (1995) required the regions of enhanced tangential wind speeds to be at least 10-km radial width and 5 m s^{-1} greater than the nearby relative minimum. Their study indicates that secondary tangential wind maxima, associated with either spiral rainbands or concentric eyewalls, are likely to be present at some stage of the TC life cycle. Although these features were evident in 85% of the storms in Samsury and Zipser, secondary maxima appeared in only 20% of the radial leg profiles and nearly half of these cases were associated with the well-known concentric eyewall cycles of Allen (1980) and Gilbert (1988).

Whatever the frequency that outer secondary maxima occur in the tangential wind field of TCs, we find that their influence in the axisymmetric vortex structure is small for the majority of individual storm cases, especially in the near-core region (1–3 RMW distances). Since secondary maxima appear to be most often associated with asymmetric features such as convective rainbands, their representation in the azimuthal-mean estimate should be greatly reduced. We have observed (not shown) that secondary tangential wind maxima present in the radial leg profiles from one or two storm quadrants are most often represented as smoothed and barely discernible disturbances in the azimuthal-mean estimate $\overline{V}$, usually 1 m s^{-1} greater than at proximate radii. In contrast, secondary maxima associated with symmetric features such as concentric eyewalls may be very pronounced in the radial profile of azimuthal-mean tangential wind.

Very few prominent secondary maxima, however, are observed between 1–3 RMW distances in this study. Close inspection of the $\overline{V}$ radial profiles for the major hurricane group in Fig. 4 reveals that the tangential wind for the vast majority of cases decreases *monotonically* with radius as $r^{-\alpha}$, where $\alpha \approx 0.5 \pm 0.1$. Although several major hurricane cases in Fig. 4 clearly possess prominent secondary maxima resulting in small estimated values of α, most cases with significant outer maxima are located *beyond* three RMW distances. This is evident in Gilbert (Fig. 12a) as well as many other cases (e.g., Allen 1980, Olivia 1994, and Luis, Marilyn, and Opal in 1995). This is consistent with the results of Samsury and Zipser (1995), who found that secondary maxima were located at an average radius of 90 km, or three RMW distances from the median primary wind maxima located at 30-km radius. In addition, all three profiles (Gilbert, Alicia, Gloria) from Fig. 2 of their study, which according to the authors' represents the variability of this structural feature, possess secondary tangential wind maxima beyond three RMW distances.

5. Discussion

According to linear VRW theory, the azimuthal-mean radial structure in the near-core region of the primary circulation plays an essential role in determining the TC vortex response to vertical wind shear. Different outcomes in the vortex response to vertical shear can be expected depending on the choice of idealized vortex profile, as demonstrated by RMG and SM1,2. For a pure Rankine vortex with core Rossby numbers

greater than unity, linear theory predicts, and numerical simulations verify, an unstable response in which the tilted vortex precesses with exponential growth in the tilt angle (SM2). For the benchmark J95 simulation, the positive radial gradient of relative vorticity at the critical radius of the S90 vortex (for a simple tilt mode) yields an unstable response in which the vortex tilt increases with time and eventually shears apart (J95; RMG). Although the critical radii for simple tilt modes were not calculated by RMG for the other J95 and Jones (2000) simulations that employ the S90 class of vortices, it is not surprising that these vortices exhibit a tendency for growing tilt, given the likelihood that the critical radius resides in the region of positive vorticity gradient. The unrealistic Rankine and S90 vortices evidently lack the girth in the tangential wind and cyclonic relative vorticity structure that is necessary to withstand weak to moderate vertical shear.

For completeness, we briefly discuss another class of idealized vortex profiles [J95; Eq. (2)] employed in a minority of the Jones' simulations for the purpose of broadening the vortex structure.[4] In support of RMG and SM1, the Jones (2000) simulation employing the NP2 vortex (see their Table 1), possessing a much broader profile shape than the S90 family of vortices, resulted in vertical coherence in the presence of moderate unidirectional vertical shear (6 m s^{-1} per 10 km). The linear VRW theory offers the simplest and most complete explanation of this particular vortex behavior: the placement of the cyclonic to anticyclonic PV transition farther out (~4 RMW; see Fig. 12 in Jones 2000) yields monotonically decreasing PV and negative radial gradient at the critical radius (RMG). The sole "broad" simulations of J95 and Jones (2004) also tended to resist vertical shear. The broad vortex employed in the J95 simulation appears to resist vertical shear by tilting over much more slowly than the other J95 simulations (that utilized S90 vortices). According to Jones (2004), the vortex tilt in this particular simulation actually decreases upon further time integration. The same broad vortex becomes even more resilient to vertical shear when the latitude is increased and the static stability reduced (Jones 2004), exhibiting comparable vertical coherence as the NP2 simulation. In contrast to the broadly shaped NP2 vortex discussed above, however, the vortex broadening here was accomplished only by increasing the RMW (from 100 to 150 km), while retaining similar shape characteristics of the S90 vortices.

The vortex behavior in the two simulations employing the "broad" vortex may at first glance appear to contradict linear VRW theory. Although the critical radii for a simple tilt mode has not been calculated for these two simulations, the shift to a region of lesser and possibly negative vorticity gradient is quite plausible in the context of linear VRW theory, in terms of the performed adjustment of environmental and/or vortex parameters (increased RMW) in those studies. Based on the theory presented in Schecter et al. (2002) and SM1, it may also be hypothesized that the growing vortex tilt in these nonlinear J95 simulations modifies the basic-state PV profile in the vicinity of the critical radius in such a way as to erode the instability and render it neutral. In any event, although the broad simulations show similar resiliency to shear as more realistic vortices, it is quite clear that vortices possessing S90-like characteristics exhibit great sensitivity to the tilt evolution.

From the perspective of dry-adiabatic dynamics, the foregoing results suggest that the near-core vortex structure outside the RMW enables TCs to withstand and survive episodes of weak to moderate vertical wind shear, in contrast to the response of the unrealistic Rankine and S90 idealized vortices discussed. The VRW predictions concerning the relationship of broadness of the primary circulation and vortex resiliency have been broadly verified in the full physics cloud-resolving numerical simulation of Hurricane Bonnie (Braun et al. 2005). Bonnie experienced moderate to strong northwesterly shear during the intensive observational period, yet remained intact and vertically coherent. Together, these results demonstrate that caution must be used in the type of idealized vortex specified in theoretical and modeling studies of TC evolution.

6. Conclusions

In this study, flight-level aircraft observations obtained from Atlantic and eastern Pacific tropical cyclones are utilized to construct hundreds of radial profiles of azimuthal-mean tangential wind and relative vorticity. Motivated by recent theoretical work examining TC resiliency, we highlight the near-core region beyond the RMW in order to reveal the true TC radial structure and to compare with some commonly used idealized vortices.

Composites of the axisymmetric primary circulation reveal that the true underlying radial structure of TCs is distinct from the idealized vortices by the relatively slow tangential wind decrease and the associated monotonic decay of cyclonic relative vorticity far beyond the RMW. Estimates of the tangential wind asymmetry further confirm that the observed broadness of the primary circulation is an intrinsic property of TCs that persists in the various storm quadrants. Although the presence of secondary tangential wind maxima may in a minority of cases enhance this broadness, the slow tangential wind decay is primarily a consequence of the axisymmetric angular momentum balance for a quasi-steady vortex subjected to quadratic drag in the boundary layer (Riehl 1963; Emanuel 1986; Pearce 1992).

[4] Only one simulation employed a vortex (termed NP1, see Table 1 of Jones 2000) possessing a similar narrow radial structure as the S90 standard vortex, and not surprisingly, similar tilt behavior.

This characteristic radial structure of real TCs guarantees *a strong negative radial gradient of vorticity at the critical radius that has recently been implicated as essential to maintaining the resiliency of the TC vortex in weak to moderately sheared environments*.

Strictly speaking, the broadness of the primary circulation observed here concerns the low to middle troposphere of TCs where the flight-level data is obtained. Comparisons of composite subgroups representing different flight levels from the same TC intensity class, in addition to several individual storm cases for which simultaneous missions occurred at different altitudes, suggest the approximate invariance of the nondimensional radial structure. In conjunction with the observed upper-level vortex structure from past studies (discussed in section 1c) we anticipate that our results hold throughout the vortex. We therefore expect that the vertically averaged vortex possesses the relevant structural characteristics necessary for vortex resiliency in weak to moderate shear, as predicted by the equivalent barotropic theory.

We believe that a complete understanding of the TC resiliency problem should lead to improvements in TC intensity forecasting. However, this further requires the understanding of the influence of the baroclinic vortex structure, in addition to the effects of moist processes and the secondary circulation. These topics will be considered in upcoming work.

Acknowledgments. This work was supported in part by U.S. Office of Naval Research under Grants N00014-021-0474 and N00014-021-0532, and National Science Foundation Grant ATM-013200. We are very grateful to Dr. Hugh Willoughby and the Hurricane Research Division for their efforts in providing the flight-level data and making this work possible. Special thanks given to Dr. Dave Schecter and Dr. Gary Barnes for their constructive comments.

APPENDIX

Idealized Tangential Wind and Vorticity Profiles

The four idealized vortex profiles discussed in this paper that represent the radial structure of the axisymmetric primary circulation are presented here in nondimensional form. The radius r, tangential wind $\overline{V}$, and relative vorticity $\overline{\zeta}$ are expressed in terms of their scales and mondimensional counterparts:

$$r = \text{RMW}\,\tilde{r},\ \overline{V} = \overline{V}_{\max}\tilde{V},\ \overline{\zeta} = \overline{\zeta}_{\max}\tilde{\zeta}.$$

The basic scales used are the *maximum azimuthal-mean tangential wind speed* $\overline{V}_{\max}$ and azimuthal-mean RMW. The scale for the relative vorticity is derived quantity, that is, $\overline{\zeta}_{\max} = \overline{V}_{\max}/\text{RMW}$. For notational convenience, the tildes are dropped in the following nondimensional equations.

a. Modified Rankine vortex

$$\overline{V}(r) = \begin{cases} r & r \le 1 \\ r^{-\alpha} & r > 1 \end{cases}, \tag{A1}$$

$$\overline{\zeta}(r) = \begin{cases} 2 & r \le 1 \\ (1-\alpha)r^{-(1+\alpha)} & r > 1 \end{cases}, \tag{A2}$$

where $0 \le \alpha \le 1$. A pure Rankine vortex, where $\alpha = 1$, is

$$\overline{V}(r) = \begin{cases} r & r \le 1 \\ r^{-1} & r > 1 \end{cases}, \tag{A3}$$

$$\overline{\zeta}(r) = \begin{cases} 2 & r \le 1 \\ 0 & r > 1 \end{cases}. \tag{A4}$$

b. Rankine-with-skirt vortex

$$\overline{V}(r) = \begin{cases} r & r \le 1 \\ \varepsilon r\left(1 - \dfrac{2r}{3\alpha}\right) + \dfrac{C_1}{r} & 1 < r \le \alpha \\ \dfrac{C_2}{r} & r > \alpha \end{cases}, \tag{A5}$$

$$\overline{\zeta}(r) = \begin{cases} 2 & r \le 1 \\ 2\varepsilon\left(1 - \dfrac{r}{\alpha}\right) & 1 < r \le \alpha, \\ 0 & r > \alpha \end{cases} \tag{A6}$$

where

$$C_1 = 1 - \varepsilon\left(1 - \frac{2}{3\alpha}\right), \quad C_2 = C_1 + \frac{\varepsilon\alpha^2}{3},$$

and $\varepsilon \ll 1$ and $\alpha > 1$. These parameters are set to $\varepsilon = 0.0498$ and $\alpha = 2$ as in SM1.

c. Gaussian vortex

$$\overline{V}(r) = \frac{1 + \sigma^{-2}}{r}[1 - \exp(-\sigma^2 r^2/2)], \tag{A7}$$

$$\overline{\zeta}(r) = (1 + \sigma^2)\exp(-\sigma^2 r^2/2) \tag{A8}$$

where $\sigma \approx 1.58520$ satisfies the transcendental relation, $\exp(\sigma^2/2) - \sigma^2 - 1 = 0$.

d. S90 vortex[A1]

$$\overline{V}(r) = \frac{C_0 r(a + 3br^4)}{(1 + ar^2 + br^6)^2}, \tag{A9}$$

$$\overline{\zeta}(r) = \frac{2C_0[a + 9br^4 - r^2(a + 3br^4)^2 + 4b^2r^{10}]}{(1 + ar^2 + br^6)^3}, \tag{A10}$$

[A1] The original tangential wind formulation from Jones (1995) was derived from the Smith (1990) streamfunction, $\psi(r) \propto (1 + ar^2 + br^6)^{-1}$. The number 3 appearing in the numerator of Eq. (A9) was incorrectly given as 5/2 in Eq. (1) of Jones (1995), resulting from a typographic error (Reasor et al. 2004). The formulation, however, was implemented correctly in the model code used in Jones (1995) (P. Reasor 2003, personal communication).

where

$$C_0 = \frac{(1 + a + b)^2}{a + 3b}.$$

As specified in Smith (1990) and Jones (1995), $a = 0.3398$ and $b = 5.377 \times 10^{-4}$.

REFERENCES

Anthes, R. A., 1982: *Tropical Cyclones: Their Evolution, Structure and Effects. Meteor. Monogr.,* No. 41, Amer. Meteor. Soc., 208 pp.

Batchelor, G. K., 1967: *An Introduction to Fluid Dynamics.* Cambridge University Press, 615 pp.

Braun, S. A., M. T. Montgomery, and Z. Pu, 2005: High-resolution simulation of Hurricane Bonnie (1998). Part I: The organization of vertical motion. *J. Atmos. Sci.,* in press.

Briggs, R. J., J. D. Daugherty, and R. H. Levy, 1970: Role of Landau damping in crossed-field electron beams and inviscid shear flow. *Phys. Fluids,* **13,** 421–432.

Croxford, M., and G. M. Barnes, 2002: Inner core strength of Atlantic tropical cyclones. *Mon. Wea. Rev.,* **130,** 127–139.

Depperman, C. E., 1947: Notes on the origin and structure of Philippine typhoons. *Bull. Amer. Meteor. Soc.,* **28,** 399–404.

Emanuel, K. A., 1986: An air–sea interaction theory for tropical cyclones. Part I: Steady-state maintenance. *J. Atmos. Sci.,* **43,** 2044–2061.

——, M. Fantini, and A. J. Thorpe, 1987: Baroclinic instability in an environment of small stability to slantwise moist convection. Part I: Two-dimensional models. *J. Atmos. Sci.,* **44,** 1559–1573.

Ford, R., 1994: The instability of an axisymmetric vortex with monotonic potential vorticity in rotating shallow water. *J. Fluid Mech.,* **280,** 303–334.

Frank, W. M., 1977: The structure and energetics of the tropical cyclone. I. Storm structure. *Mon. Wea. Rev.,* **105,** 1119–1135.

Franklin, J. L., S. J. Lord, S. E. Feuer, and F. D. Marks Jr., 1993: The kinematic structure of Hurricane Gloria (1985) determined from nested analyses of dropwindsonde and Doppler radar data. *Mon. Wea. Rev.,* **121,** 2433–2451.

Gent, P. R., and J. C. McWilliams, 1986: The instability of barotropic circular vortices. *Geophys. Astrophys. Fluid Dyn.,* **35,** 209–233.

Gray, W. M., and D. J. Shea, 1973: The hurricane's inner core region. II. Thermal stability and dynamic characteristics. *J. Atmos. Sci.,* **30,** 1565–1576.

Hoskins, B. J., M. E. McIntyre, and A. W. Robertson, 1985: On the use and significance of isentropic potential vorticity maps. *Quart. J. Roy. Meteor. Soc.,* **111,** 877–946.

Hughes, L. A., 1952: On the low-level wind structure of tropical storms. *J. Meteor.,* **9,** 422–428.

Jones, S. C., 1995: The evolution of vortices in vertical shear: Initially barotropic vortices. *Quart. J. Roy. Meteor. Soc.,* **121,** 821–851.

——, 2000: The evolution of vortices in vertical shear. II: Large-scale asymmetries. *Quart. J. Roy. Meteor. Soc.,* **126,** 3137–3159.

——, 2004: On the ability of dry tropical-cyclone-like vortices to withstand vertical shear. *J. Atmos. Sci.,* **61,** 114–119.

Jorgensen, D. P., 1984: Mesoscale and convective-scale characteristics of mature hurricanes. Part I: General observations by research aircraft. *J. Atmos. Sci.,* **41,** 1268–1285.

Kossin, J. P., and M. D. Eastin, 2001: Two distinct regimes in kinematic and thermodynamic structure of the hurricane eye and eyewall. *J. Atmos. Sci.,* **58,** 1079–1090.

——, and W. H. Schubert, 2001: Mesovortices, polygonal flow patterns, and rapid pressure falls in hurricane-like vortices. *J. Atmos. Sci.,* **58,** 2196–2209.

Malkus, J. S., and H. Riehl, 1960: On the dynamics and energy transformation in steady-state hurricanes. *Tellus,* **12,** 1–20.

Mallen, K. J., 2004: Re-examining tropical cyclone near-core radial structure from flight-level aircraft observations: Implications for vortex resiliency and intensification. M.S. thesis, Dept. of Meteorology, University of Hawaii at Manoa, 125 pp.

McWilliams, J. C., L. P. Graves, and M. T. Montgomery, 2003: A formal theory for vortex Rossby waves and vortex evolution. *Geophys. Astrophys. Fluid Dyn.,* **97,** 275–309.

Merrill, R. T., 1984: A comparison of large and small tropical cyclones. *Mon. Wea. Rev.,* **112,** 1408–1418.

Miller, B. I., 1967: Characteristics of hurricanes. *Science,* **157,** 1389–1399.

Montgomery, M. T., and B. F. Farrell, 1992: Polar low dynamics. *J. Atmos. Sci.,* **49,** 2484–2505.

——, and R. J. Kallenbach, 1997: A theory of vortex Rossby-waves and its application to spiral bands and intensity changes in hurricanes. *Quart. J. Roy. Meteor. Soc.,* **123,** 435–465.

——, V. A. Vladimirov, and P. V. Denissenko, 2002: An experimental study on hurricane mesovortices. *J. Fluid Mech.,* **471,** 1–32.

Nolan, D. S., and M. T. Montgomery, 2002: Nonhydrostatic, three-dimensional perturbations to balanced, hurricane-like vortices. Part I: Linearized formulation, stability, and evolution. *J. Atmos. Sci.,* **59,** 2989–3020.

OFCM, 1993: National hurricane operations plan. Office of the Federal Coordinator for Meteorological Services and Supporting Research, 125 pp. [Available from Office of the Federal Coordinator for Meteorological Services and Supporting Research, Suite 1500, 8455 Colesville Rd., Silver Spring, MD 20910.]

Ooyama, K., 1969: Numerical simulation of the life cycle of tropical cyclones. *J. Atmos. Sci.,* **26,** 3–40.

Orr, W. M., 1907: The stability or instability of the steady motions of a perfect liquid and of a viscous liquid. *Proc. Roy. Irish Acad.,* **A27,** 9–138.

Papaloizou, J. C. B., and J. E. Pringle, 1987: The dynamical stability of differentially rotating discs—III. *Mon. Not. Roy. Astron. Soc.,* **225,** 267–283.

Pearce, R. P., 1993: A critical review of progress in tropical cyclone physics including experimentation with numerical models. *Proc. ICSU/WMO Int. Symp. on Tropical Disasters,* Beijing, China, ICSU/WMO, 45–59.

Petrova, L. I., 1995: Radial structure of tangential wind in a tropical cyclone as derived from observational data. *Russ. Meteor. Hydrol.,* **3,** 1–8.

Plougonven, R., and V. Zeitlin, 2002: Internal gravity wave emission from a pancake vortex: An example of wave–vortex interaction in strongly stratified flows. *Phys. Fluids,* **14,** 1259–1268.

Reasor, P. D., and M. T. Montgomery, 2001: Three-dimensional alignment and corotation of weak TC-like vortices via linear vortex Rossby waves. *J. Atmos. Sci.,* **58,** 2306–2330.

——, F. D. Marks, and J. F. Gamache, 2000: Low-wavenumber structure and evolution of the hurricane inner core observed by airborne dual-Doppler radar. *Mon. Wea. Rev.,* **128,** 1653–1680.

——, ——, and L. D. Grasso, 2004: A new look at the problem of tropical cyclones in vertical shear flow: Vortex resiliency. *J. Atmos. Sci.,* **61,** 3–22.

Riehl, H., 1954: Tropical storms. *Tropical Meteorology,* McGraw-Hill, 281–357.

——, 1963: Some relations between wind and thermal structure of steady state hurricanes. *J. Atmos. Sci.,* **20,** 276–287.

Rotunno, R., and K. A. Emanuel, 1987: An air–sea interaction theory for tropical cyclones. Part II: Evolutionary study using a nonhydrostatic axisymmetric numerical model. *J. Atmos. Sci.,* **44,** 542–561.

Samsury, C. E., and E. J. Zipser, 1995: Secondary wind maxima in hurricanes: Airflow and relationship to rainbands. *Mon. Wea. Rev.,* **123,** 3502–3517.

Schecter, D. A., and M. T. Montgomery, 2003: On the symmetrization rate of an intense geophysical vortex. *Dyn. Atmos. Oceans,* **37,** 55–88.

——, and ——, 2004: Damping and pumping of a vortex Rossby wave in a monotonic cyclone: Critical layer stirring versus inertia–buoyancy wave emission. *Phys. Fluids,* **16,** 1334–1348.

——, ——, and P. D. Reasor, 2002: A theory for the vertical alignment of a quasigeostrophic vortex. *J. Atmos. Sci.,* **59,** 150–168.

Schubert, W. H., M. T. Montgomery, R. K. Taft, T. A. Guinn, S. R. Fulton, J. P. Kossin, and J. P. Edwards, 1999: Polygonal eyewalls, asymmetric eye contraction, and potential vorticity mixing in hurricanes. *J. Atmos. Sci.,* **56,** 1197–1223.

Shapiro, L. J., and M. T. Montgomery, 1993: A three-dimensional balance theory for rapidly rotating vortices. *J. Atmos. Sci.,* **50,** 3322–3335.

——, and J. L. Franklin, 1995: Potential vorticity in Hurricane Gloria. *Mon. Wea. Rev.,* **123,** 1465–1475.

Shea, D. J., and W. M. Gray, 1973: The hurricane's inner core region. I. Symmetric and asymmetric structure. *J. Atmos. Sci.,* **30,** 1544–1564.

Sheets, R. C., 1980: Some aspects of tropical cyclone modification. *Aust. Meteor. Mag.,* **27,** 259–280.

Smith, R. K., 1990: A numerical study of tropical cyclone motion using a barotropic model. I: The role of vortex asymmetries. *Quart. J. Roy. Meteor. Soc.,* **116,** 337–362.

Thomson, W. W., 1887: Stability of fluid motion: Rectilinear motion of viscous fluid between two parallel plates. *Philos. Mag.,* **24,** 188–196.

Thorpe, A. J., 1985: Diagnosis of balanced vortex structure using potential vorticity. *J. Atmos. Sci.,* **42,** 397–406.

Weatherford, C. L., 1989: The structural evolution of typhoons. Dept. of Atmospheric Sciences Paper 446, Colorado State University, 198 pp.

Willoughby, H. E., 1990a: Temporal changes of the primary circulation in tropical cyclones. *J. Atmos. Sci.,* **47,** 242–264.

——, 1990b: Gradient balance in tropical cyclones. *J. Atmos. Sci.,* **47,** 265–274.

——, 1991: Reply. *J. Atmos. Sci.,* **48,** 1209–1212.

——, and M. B. Chelmow, 1982: Objective determination of hurricane tracks from aircraft observations. *Mon. Wea. Rev.,* **110,** 1298–1305.

——, and M. E. Rahn, 2004: Parametric representation of the primary hurricane vortex. Part I: Observations and evaluation of the Holland (1980) model. *Mon. Wea. Rev.,* **132,** 3033–3048.

——, J. A. Clos, and M. G. Shoreibah, 1982: Concentric eyewalls, secondary wind maxima, and the evolution of the hurricane vortex. *J. Atmos. Sci.,* **39,** 395–411.